submitted to **International Federation of Automatic Control, CAMS'92,** Genova, Italy, 8-10 April 1992

COORDINATED VEHICLE/MANIPULATOR DESIGN AND CONTROL ISSUES FOR UNDERWATER TELEMANIPULATION

Hagen Schempf and Dana R. Yoerger[1]
Carnegie Mellon University
Robotics Institute - Field Robotics Center
5000 Forbes Ave., Pittsburgh, PA 15213, USA

ABSTRACT

Control of underwater vehicle/manipulator systems described by highly nonlinear and coupled dynamics can be improved through careful vehicle and manipulator design, while novel controller structures can improve system performance and simplify the man/machine interface requirements. Understanding and overcoming sensor limitations present in underwater vehicle navigation is one of the basic requirements for high fidelity control and trajectory planning of the manipulators' endeffector attached to its mobile base. Modelling and control of ducted propellers used as actuators becomes crucial for fine control and the avoidance of limit-cycling during hovering maneuvers. The ability to model the pitch/roll-translation coupling for such systems is necessary to increase the performance and fidelity of trajectory following and force/impedance control. Neglecting such coupling effects not only results in poor tracking performance but can also cause instabilities due to excitation of unmodelled 'pendulum' modes and the operation near vehicle/manipulator singularities. The necessity to coordinate vehicle and manipulator control for unconstrained motions and contact tasks requires the development of a coordinated controller structure. The use of a dual impedance structure can insure stability during contact tasks with a wide variety of environments, while the use of a coupling impedance is used to shape the relative behavior between vehicle and manipulator endpoint. The operational use of such a dual/coupled controller structure extends the maneuvering and manipulation capabilities of mobile manipulation platforms by reducing the number of variable controller parameters and thus operator burden while increasing system flexibility and userfriendliness of the man/machine interface. This paper presents preliminary simulation and experimental results.

I. INTRODUCTION

The use of manipulators on maintenance, recovery, and research ROVs has become standard practice. Such systems are usually controlled separately, in that there is a separate vehicle control joystick and another joystick/kinematic master to control the manipulator. The operational scenario usually involves getting to the work site and invoking a depth and/or heading servo on the vehicle so that the operator is free to concentrate on operating the robot arm. Other implementations may use a second arm to attach to a structure in order to stabilize the workplatform. This approach is usually not very common in research or recovery missions for ROVs, since there usually is no large fixed object to brace the vehicle against. The vehicle is usually required to free-float and compensate/coordinate motions with the manipulator.

Working off a mobile base which is gravity/buoyancy stabilized, while interacting with the environment, is not a very simple task. Not only will one need to coordinate vehicle and manipulator motions, but also the design of vehicle and manipulator have to be well thought out, as the inherent system dynamics may yield poor performance ('wobbly' base, swaying endeffector motions) and result in a poorly behaved or even unstable manipulator endeffector response.

The more recent design research and implementations for underwater vehicles [Schempf 1986], for use as camera platforms (JASON JUNIOR 1985) as well as manipulation platforms (JASON DESIGN 1988), have clearly stressed the important issues relevant to underwater vehicle design. Understanding such factors as (1) pitch/roll stabilization via metacentric height adjustments, (2) location of center of thrust and thrust allocation, (3) hydrodynamic cross-sections and center of drag, is important in the design of a stable workplatform, be it for imaging or manipulation tasks. The success of these designs for imaging purposes, was clearly illustrated in the 1986 TITANIC exploration with JASON Jr., and the last two JASON PROJECT explorations into the Mediterranean and Lake Ontario. In the last two cases, we were able to obtain clear and stable video images, while using additional sensors to accurately locate and identify archeologically valuable artifacts (amphoras, shipwreck outline, canons, masts, etc.) on two different shipwrecks (Roman shipwreck 400 A.D., and the Hamilton & Scourge from the Civil War). The quality of the video is substantially improved over that of other systems used for such tasks (AMUVS, Benthos RPV).

Manipulation off a platform such as JASON was also shown to be very successful, as the damageless recovery of 30 amphorae from 400 A.D., and biological and geological specimen

1: Deep Submergence Laboratory, Woods Hole Oceanographic Institution, Woods Hole, MA 02543, USA

from underwater 'smokers', have attested to. Not only vehicle design, but also careful manipulator and endeffector design proved to be crucial in this mission [DiPietro 1988, Yoerger et al 1989]. Designing a manipulator arm for dexterous and fine manipulation was necessary to be able to handle such delicate objects. Proper selection of motors and transmissions and sensors, including the proper control laws were all essential components of a successful implementation of a complete manipulation design and strategy, yielding a manipulator with superior performance, compared to other commercially available manipulators [Yoerger et al 1990, Schempf et al 1992].

The standard stiff position servos implemented on underwater electric and electro-hydraulic manipulators are not always sufficient to provide for fine, high dexterity and accurate control, where bandwidth and stability are important task performance criteria. Force-reflecting master/slave manipulators solve part of the problem, but deadbands, force thresholds and bandwidth limitations are again not always sufficient to yield acceptable performance. Insuring stability during interactive tasks, and good trajectory following can be accomplished with an impedance controller structure [Hogan 1985]. The use of such schemes has been proven to work very well on many stationary manipulators [Andrews 1983, Salisbury 1980], since it can be easily implemented in cartesian or task space, yielding desired spring-like and viscous damping behavior, with adjustable effective endpoint inertia. This approach gives the operator the ability to set desired behaviors which may be appropriate for different tasks. Prying a rock loose from an abatement may require 'stiff' joints (large stiffness and apparent mass), while handling an amphora or biological specimen would require a 'soft' apparent endpoint behavior (low stiffness, light apparent mass). We will show that this control technique can also be used to coordinate vehicle and manipulator motions, thereby combining stable control, endpoint behavior modulation and motion planning into a single structure. This approach extends the capabilities and handles provided by earlier task resolved controller designs [Yoerger & Slotine 1987].

Implementing such a stiffness or impedance control scheme on a manipulator mounted on a mobile base requires not only good knowledge of the dominant system dynamics (as they are rarely negligible), but also the restructuring of the control algorithm in order to coordinate vehicle and manipulator motions while insuring stability. Structuring the controller so as to yield the maximum performance versatility and ease of operation will result in a more operationally capable system. The complexity of the man/machine interface can be reduced from several physical system-specific input devices, to a single joystick or kinematic master, if a certain controller structure is selected with a minimal yet necessary set of controllable controller parameters.

This paper will first explore the important vehicle design and control issues involved in the design of a highly controllable workplatform. Constraints such as actuator and sensor limitations will be highlighted in order to understand and compensate for nonlinearities in pure vehicle control tasks. This will then be complemented by the study of the complex dynamics that dominate the dynamics of pitch/roll-translation for mobile underwater manipulation platforms. Modelling the coupled dynamics is necessary as even the best designed vehicle will pitch/roll and thus result in manipulator endpoint translations which have to be compensated for. The better our model of this physical system is, the better we can predict behavior and thus try to compensate for it. We will then explore the usefulness of the standard impedance and stiffness controller for redundant vehicle/manipulator systems and motivate the need for a modified impedance controller structure. The importance of proper dynamic modelling will become apparent when we compare the performance differences for different assumed model structures. A discussion of the important operational scenarios and criteria will also be given, in order to explain the ease and usefulness of such an implementation, while exploring the issues involved in controller parameter selection, as well as the implementation in simple task scenarios.

II. VEHICLE DESIGN AND CONTROL ISSUES

• *Vehicle Design Parameters (System Layout, Actuators and Sensors)*

The physical layout of the vehicle can have a very large impact on vehicle behavior [Schempf 1986, Yoerger et al 1986, DSL Design Team 1987]. The open-loop dynamics of the vehicle will have to be chosen so as to eliminate/reduce behaviors that are difficult to modify through feedback control and any available actuators. Vehicle pitch and roll have to be as passively stable as possible, by increasing the metacentric height (distance between the vehicle's center of gravity and center of buoyancy), which according to the simple pendulum's natural frequency equation $\omega = \sqrt{g/z_{cb-cg}}$ determines the frequency of oscillation [Tanaka et al 1985, Yoerger et al 1986, Schempf 1986]. The relation governing the maximum expected pitch/roll for a certain applied moment is

$$M_t + M_h = W z_{cb-cg} \sin\phi \qquad (1)$$

where:

M_t=Moment due to thruster(s)
M_h=Moment due to hydrodynamic effects
W= Dry Weight of the vehicle
z_{cb-cg}=Metacentric Height
ϕ=Pitch or Roll Angle

as shown in Eqn. 1. The applied moment M_t, can be upper-bounded by the moment created by the saturation thrust delivered by the forward/sideways thrusters, multiplied by the separation distance between center of thrust and the center of gravity. Keep in mind, that even if the center of thrust was perfectly aligned with the center of mass, the vehicle would still exhibit pitch/roll-translation coupling, due to the distributed added mass effects and the variable location of the net center of drag (captured by the term M_h).

Active control over these oscillatory modes can be obtained by proper placement of thrusters in a top-view triangular arrangement. The actuator saturation and geometrical characteristics really only allow for a limited amount of control, such as in aiding to damp out oscillations, but not to completely compensate for large pitch/roll excursions, because of external payload addition or coupling from an anchored manipulator exerting large forces. Careful placement of the thrusters is important, as it can minimize the pitch/roll-translation coupling due to the interactions of the center of thrust, center of drag and center-of-mass/center-of-thrust locations.

Ducted propellers driven by brushless DC motors, represent quite a nonideal actuator. Axial and cross-flows diminish thruster efficiency drastically, hampering control and maneuverability in the presence of any sizeable current.

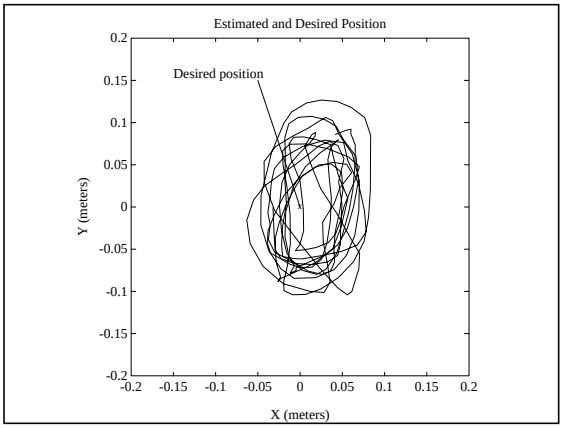

Figure 1: Limit-cycle phenomenon in a hovering ROV

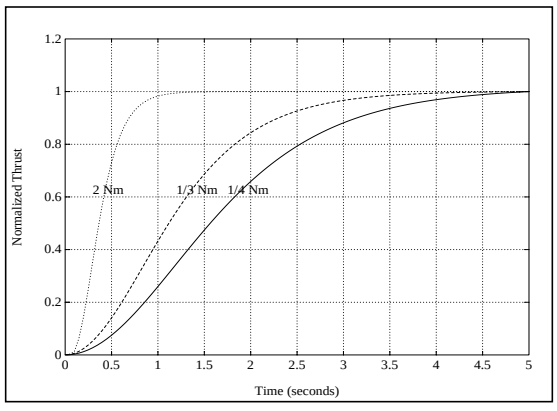

Figure 2: Nonlinear Thruster Characteristics

Seal- and motor-bearings affect the low-end thrust of the thruster, and cause the onset of 'hunting' during hovering maneuvers, akin to a steady limit-cycle about the desired position and heading (see Figure 1). It has been shown [Yoerger et al 1990], that the thruster behaves like a sluggish nonlinear filter, where the speed of response depends on the commanded thrust level (see Figure 2). A simple analysis showed that this results in a severe bandwidth limitation and causes limit cycles. The use of an adaptive sliding controller resulted in increased thruster fidelity and compensation for uncertainties in parameters and thruster degradation (broken prop. blade, fouling, etc.). The use of a model that parametrizes the thrust force as being proportional to the applied motor torque and the abs-square of the prop speed ($\omega|\omega|$), yields a structure that lent itself to an adaptive control and identification scheme. Performance improvements in hovering fidelity were achieved using this novel thruster model and adaptive controller.

The usual suite of sensors for underwater vehicles includes accelerometers, angular position and rate inclinometers, gyros, and depth and 3D acoustic positioning sensors. Heading and heading rate are usually measured by a flux-gate compass and a directional gyro. Heading measurements can be augmented and supported by placing two acoustic transponders separated along the vehicle and interrogating them within a high accuracy acoustic positioning net. Accuracies for a commercially available acoustic positioning net (SHARPS) can be as good as a few millimeters over a 120 meter range. This high frequency (300 kHz) acoustic system can deliver updates at about 10 Hz over its entire range. Accurate vehicle position updates are crucial in fine and high bandwidth vehicle and mobile manipulator control. The acoustic noise levels present at a certain work site can be 'filtered' without affecting update rate and accuracy. Blending all these independent and complimentary sensors is part of sensor fusion research currently underway, offering a good means of accounting for individual sensor accuracy, noise level, update rate and frequency response. A simple example would be the measurement of vehicle heading. One can blend the gyro (heading rate) measurements with that of the SHARPS (heading angle) system, by using a first order complimentary filter which produces a heading estimate that blends the accurate high frequency rate measurements of the gyro with those measurements from the accurate low frequency drift-free SHARPS system.

A drawing of the JASON system (Figure 3) illustrates the synthesis of many design criteria mentioned earlier. The shape and location of the flotation (syntactic foam), the location and distribution of vehicle components (weight distribution), the number and location of thrusters, and the location of acoustic transponders reflect some of the design decisions implemented in this remotely operated vehicle

platform.

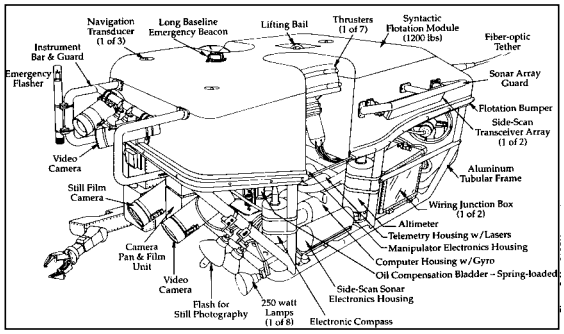

Figure 3: Layout View of JASON ROV

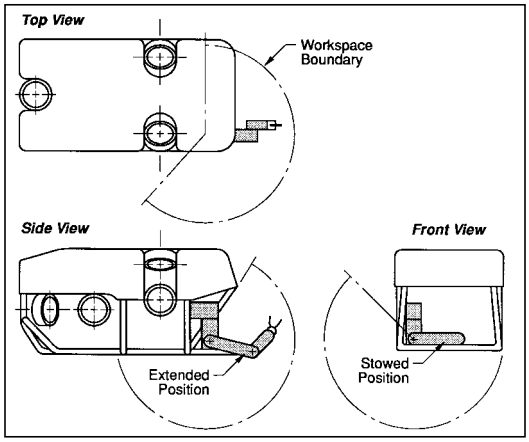

Figure 4: Plan Views of JASON's manipulator workspace

The attached manipulator arm was carefully placed with payload balancing and maximum available workspace in mind (see Figure 4). The importance of incorporating the manipulator into the kinematic and dynamic system model will be dealt with a bit later on in this paper, at which point we will illustrate the necessity and advantages to be gained.

• *Nonlinear Vehicle Dynamics*

Precise, reliable, and high bandwidth control of an underwater vehicle requires the synthesis of solutions to challenging problems in vehicle design, sensing, dynamic modelling and control system design. The dynamics of such systems are very hard to characterize deterministically for several reasons. Physically, the usually unstreamlined, non-hydrodynamic shape of these vehicles, results in hydrodynamic drag and added/effective mass effects which are difficult to model. A model structure is based mainly on empirically derived relations, such as the abs-square drag law ($u|u|$) with a variable drag coefficient or the acceleration-dependent added mass term, and even then such nonlinear expressions have parameters that are not fixed, but vary as a function of many other parameters. The most commonly used nonlinear model

$$\Sigma \vec{F} = \hat{\underline{M}}_e \ddot{\vec{x}} = \hat{\alpha} \vec{F}_u - \hat{\underline{C}}_d \dot{x}|\dot{x}| + \hat{\underline{F}}_d \qquad (2)$$

where:

F_u=Actuator Thrust
F_d=Disturbance Forces (currents, tether,...)
C_d=Drag Coefficient
M_e=Effective Inertia Tensor
α=Actuator Gain
x=Linear Displacement

structure is shown in Eqn.2, using Newton's laws to express the behavior of the vehicle as a function of best-estimate parameters (denoted by '^') in the drag term C_d, the effective mass M_e, the disturbance F_d, and the actuator gain α. Bounding the uncertainty in the knowledge of these terms as well as that of the disturbance-term F_d, can be effectively used in sliding control [Slotine 1985], to design a robust controller and thus improve overall system performance without the need for time and money-consuming hydrodynamic modelling and the subsequent design of gain-scheduling controllers. Performance in closed-loop trials has been shown to be better and more robust than with other standard controller structures. Figure 5 illustrates this point by showing a top-view of a closed-loop rectangular trajectory-following task for the BENTHOS ROV.

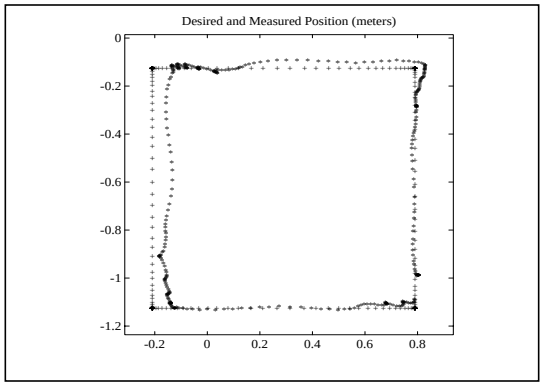

Figure 5: Closed-loop ROV trajectory following performance

More recent work [Yoerger 1990, 1991] has also shown that one can use adaptive techniques to continuously update estimates of effective mass, actuator gain, disturbances, and drag coefficient, as denoted in Eqn.3 by the time-variation symbol 't', to improve system performance and even obtain better physical estimates of these parameters.

$$\hat{\underline{M}}_e(t)\ddot{\vec{x}} = \hat{\alpha}(t)\vec{F}_u - \hat{\underline{C}}_d(t)\dot{x}|\dot{x}| + \hat{\underline{F}}_d(t) \qquad (3)$$

Shown in figure 6, we can illustrate adaptation convergence for the different parameters (added mass, drag coefficient, actuator gain) through a single error-metric plot. Sliding control methodologies [Yoerger and Slotine, 1988] will insure that adaptation will force the error-metric to eventually remain within deterministic boundaries, as shown in figure 6. This approach represents a viable solution to operations in highly variable underwater currents, or scenarios where disturbances due to tether drag are not uncommon nor negligible. Since we simplified the hydrodynamics of the system, neglecting

vortex shedding and past fluid flow history, we can at least expect, if properly bounded, that the ensuing disturbances can be compensated for in an optimum and robust fashion. A discrete nonlinear implementation of the above system dynamics and subsequent controller development are treated in detail by Delonga [1987].

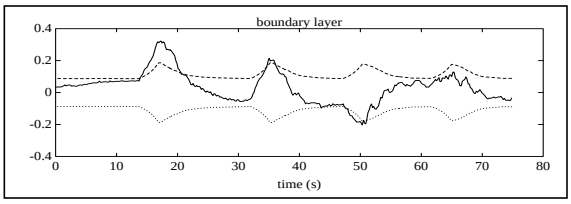

Figure 6: Convergence of error-metric 's' to within achievable boundaries..

III. VEHICLE - MANIPULATOR DYNAMICS

In order to understand the complexities involved in the dynamics and control issues of vehicle/manipulator systems, consider the system depicted in Figure 7. We have shown a vehicle and its manipulator as a 3-dimensional system, with 5 degrees of freedom. The vehicle is allowed to translate forward and in reverse, change vertical position up and down, while allowing for pitching motions. The 2 DOF manipulator remains in the *uw*-plane described by the vehicle coordinates. Notice that the translational vehicle velocities are described in a body-referenced frame. We have limited ourselves to such a system in order to illustrate the problems one encounters while attempting to design a controller for such a highly coupled system.

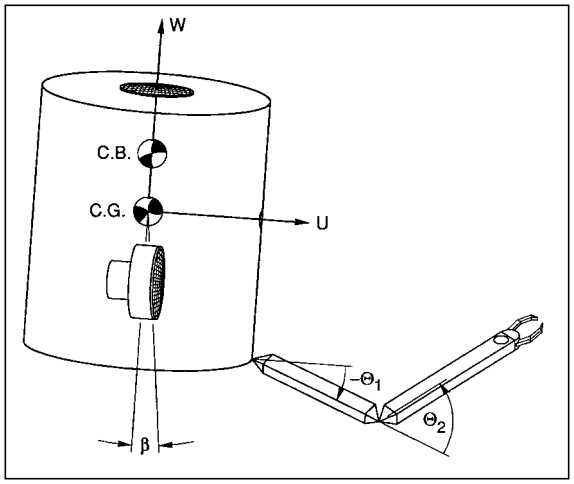

Figure 7: Vehicle/Manipulator System with 5 degrees of freedom moving in the vertical plane.

The complexity of the model can be increased by including another set of coupled/uncoupled equations to study the roll/translation dynamics. We will limit ourselves in this study to pitch-translation coupling.

The physical system can now be modelled by a set of parameters to be used in the Lagrangian expression in order to derive the equations of motion using the required set of generalized coordinates.

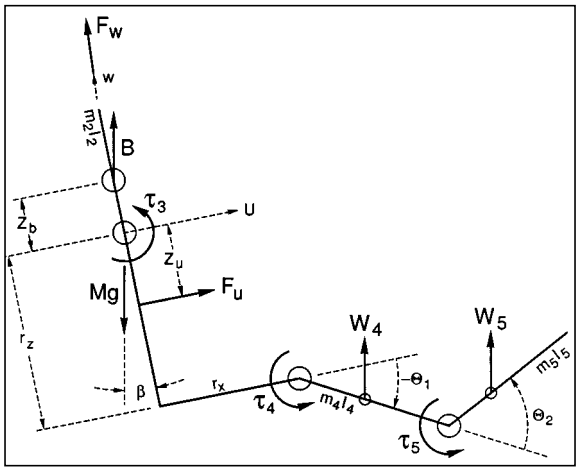

Figure 8: Parametric stick-figure showing modelling parameters.

Figure 8 illustrates these in a stick figure with parameters and variables necessary to assemble the Lagrangian, which consists of kinetic and potential co-energy terms:

$$L=T^{*} - U, \text{ where}$$

$$\text{and, } U = \sum_{i=1}^{n} m_i \vec{g}^{T} r_{o,ci} \qquad (4)$$

Using body-referenced vehicle translation velocities u and w, vehicle pitch angle β and rate q, and the manipulator coordinate angles θ_1 and θ_2 with rates $\delta(\theta_1)/dt$ and $\delta(\theta_2)/dt$ as the generalized coordinates Θ, we can formulate the Lagrangian energy terms. Using the rules for generating the individual equations of motion

$$\frac{d}{dt}\frac{\partial L}{\partial \dot{\Theta}_i} - \frac{\partial L}{\partial \Theta_i} = Q_i \ldots i = 1, \ldots, n \qquad (5)$$

we arrive at a set of equations, which in vector for can be written as:

$$\underline{H}(\vec{\Theta})\,\ddot{\vec{\Theta}} + \vec{h}(\dot{\vec{\Theta}}, \vec{\Theta}, t) = \vec{\tau}$$

$$where \ldots \dot{\vec{\Theta}} = \begin{bmatrix} u & w & q & \dot{\theta}_1 & \dot{\theta}_2 \end{bmatrix}^{T} \qquad (6)$$

The individual components of the inertia tensor $\underline{H}(\vec{\Theta})$, are made up of the individual inertia terms as well as several cross-coupling

terms, which result in a symmetric matrix. In order to understand that even in the inertia tensor the cross-coupling effects are not negligible, we analyzed the absolute magnitude representation of the individual elements of the inertia matrix (assumes sin(?)~1 and cos(?)~1), which represent the coupling of the vehicle accelerations (u, v, q) and the manipulator (θ_1, θ_2). Remember that the linear manipulator endpoint accelerations are influenced by the angular accelerations of the vehicle ($H_{(1,2)3}$), as well as the joint accelerations ($H_{(1,2)(4,5)}$), and vice versa. Depending on the physical parameters m_4, m_5, l_4, l_{c4}, l_5 and l_{c5}, the cross-coupling effects will vary in magnitude. If we assume that for a typical underwater vehicle/manipulator system, the inertia ratio M/m lies around 20:1, with a workspace of about 2 meters, and vehicle dimensions such that $r_x=r_z=1$ meter, we can get a matrix scaling effect such that the inertia matrix magnitudes can be numerically expressed as:

$$\underline{H} \cong M \begin{bmatrix} 1.1 & 0 & 0.2 & 0.1 & 0.025 \\ 0 & 1.1 & 0.2 & 0.1 & 0.025 \\ 0.2 & 0.2 & 1.45 & 0.45 & 0.225 \\ 0.1 & 0.1 & 0.45 & 0.213 & 0.2 \\ 0.025 & 0.025 & 0.225 & 0.2 & 0.075 \end{bmatrix} \quad (7)$$

Notice that the coupling magnitudes between translation and pitch motions are quite pronounced. Coupling between linear accelerations and rotary manipulator-link accelerations can also be quite substantial. The above analysis thus illustrates that including these modes into the overall system dynamics is well justified and that they should thus be incorporated into the controller design to yield improved performance and bandwidth.

The nonlinear cross-coupling terms assembled in $\underline{R}\left(\dot{\bar{\Theta}}, \bar{\Theta}\right)$ contain multiplicative terms in $u\dot{\theta}_1, u\dot{\theta}_2, w\dot{\theta}_1, w\dot{\theta}_2, q\dot{\theta}_1, q\dot{\theta}_2, \dot{\theta}_1^2, \dot{\theta}_2^2, \dot{\theta}_1\dot{\theta}_2, q^2, uq, wq$, and thus represent coupling terms whose magnitudes can also be shown to introduce substantial cross-coupling dynamics into all degrees of freedom. Ignoring the uq, wq, q^2, and $q\theta_{1,2}$ terms that show up in the equations for the manipulator link dynamics, could reduce closed-loop performance (bandwidth) and even represent a source of instability in a controller design which omits this coupling at the modelling stage.

The generalized forcing terms τ, are comprised of not only the actuator efforts F_u and F_w, but also the buoyancy restoring torque due to a nonzero metacentric height, and the effective drag terms on the vehicle and manipulator link geometries [Schempf 1986]. At this point the possibility to add active pitch control to the vehicle to offset the coupling of the fore/aft thruster moment about the center of gravity ($F_u z_u$), offers a possibility for the study in actuator placement, saturation characteristics and cost/performance trade-offs.

The entire details of the equations of motion are omitted here, since the actual goal of this paper is to study the use of different controller structures and their effect on closed-loop performance. The importance of this derivation, lies in emphasizing the retention of those terms that are not negligible, since they are responsible for the coupling dynamics that dominate the behavior of closed loop controlled vehicle/manipulator systems (see [Schempf 1987] for a more detailed analysis).

IV. CONTROLLER STRUCTURES

We have analyzed and experimentally compared several different controller structures which were designed and implemented separately for a vehicle and its manipulator. The performance was many times limited due to vehicle/manipulator interactions, and the combination of vehicle servoing and active joystick control of the manipulator was quite cumbersome and did not always result in desirable performance. A more complex yet beneficial controller structure was then proposed and can best be represented by the drawing in Figure 9. It shows an underwater vehicle/manipulator robot, with desired endpoint and vehicle behaviors w.r.t. the desired position represented as springs. Notice that we now have a controller that will attempt to control the endpoint of the manipulator and a fictitious vehicle point - termed the 'focal point' here - to track a desired trajectory indicated by x_d, y_d, and z_d which are cartesian positions, represented by the vector $\underline{X}_o$. A single controller is thus capable of controlling all subsystems, with behaviors that are described by the desired closed-loop system descriptors such as stiffness, damping, and inertia.

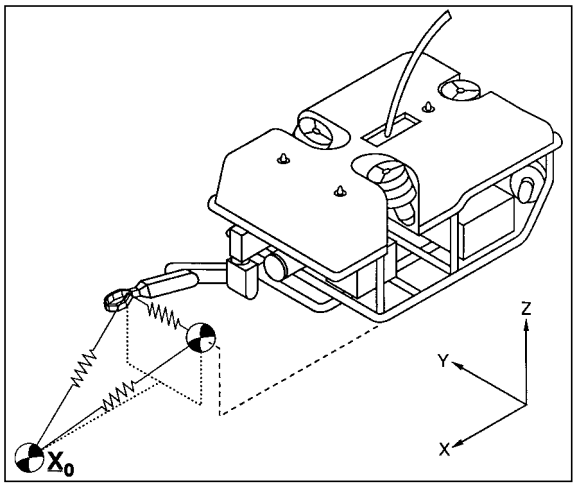

Figure 9: Coupling Impedance Controller Structure for an underwater vehicle/manipulator system.

Proper selection of these controller parameters and the respective location of the 'focal point' could allow for all possible desired vehicle and endeffector behaviors necessary to accomplish a certain task. The importance of including the proper system model into the controller was explored by simulating the 5 DOF system of Figure 7, and including in the

controller different levels of model sophistication. The analysis covers three different types of controller structures; the first which treats manipulator and vehicle as two completely separate and un-coupled systems, the second which incorporates coupled dynamics, but does not attempt to coordinate vehicle nor manipulator responses, and lastly a complete controller structure like the one in Figure 9 with knowledge of the coupling dynamics. All simulations were run with about a 25% error in model parameters, and with response bandwidths typical to the systems being analyzed (vehicle ~ 1-2 Hz, and manipulator ~ 10-15 Hz). The simulation results are graphically depicted to highlight system behavior more clearly.

• *Decoupled, reduced-order controllers*

If two separate controllers were implemented on a vehicle/manipulator system, and tuned to maximize the performance of their respective platforms, one can show that performance and even stability can be compromised in a coordinated motion. To illustrate this argument, one can command a parallel trajectory to the manipulator and vehicle and then implement those controllers, with results as shown in Figure 10.

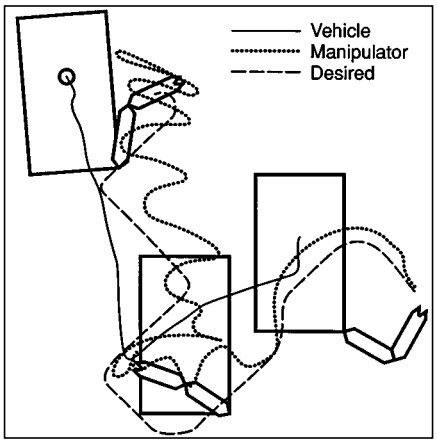

Figure 10: Performance using a controller without knowledge of coupled dynamics nor singularities

Notice the low-pass filtered response of the vehicle, coupled with excessive tracking errors for the manipulator endpoint due to pitch-translation interactions, and the constant crossing of singularity configurations of the manipulator, resulting in extremely undesirable system response. Depicted in Figure 10 are the starting, ending, and intermediate configurations of the vehicle/manipulator system. Based on this suboptimum response, one would conclude that the first improvement should be sought by including knowledge of the coupled dynamics within the controller and thus attempt to compensate for them - the approach taken and illustrated next.

• *Decoupled high-order controllers*

We have increased the controller complexity by incorporating in each separate controller knowledge about the coupling and the resulting forces/torques generated due to the interactions. As one would expect, the highly oscillatory behavior due to pitch/translation interactions has been removed, yet the trajectory tracking is still not satisfactory, which can be traced to the continuous proximity of the manipulator to its singular configurations - notice that it even reaches 'into' the vehicle, which is obviously not desirable (see Figure 11).

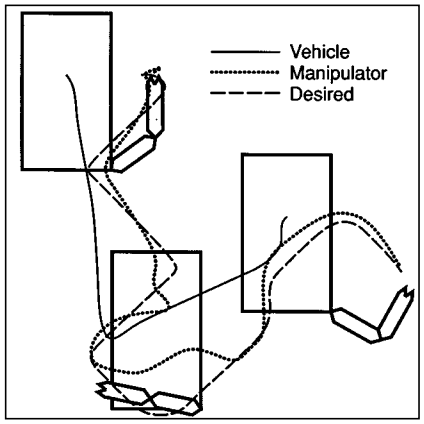

Figure 11: Performance using a controller with knowledge of coupled dynamics but without the ability to compensate for singularities.

We have now established the proper motivation for the controller structure shown in Figure 9, with the characteristic performance outlined next.

• *Coupled impedance controller*

The selected controller structure allows for a single controller to control both subsystems based on a desired trajectory to be followed by the vehicle and the manipulator endpoint. This controller structure need not know about the coupled dynamics to work properly, but its performance and stability margin are vastly improved if the coupling dynamics are included explicitly. The performance of the coupled system is depicted in Figure 12.

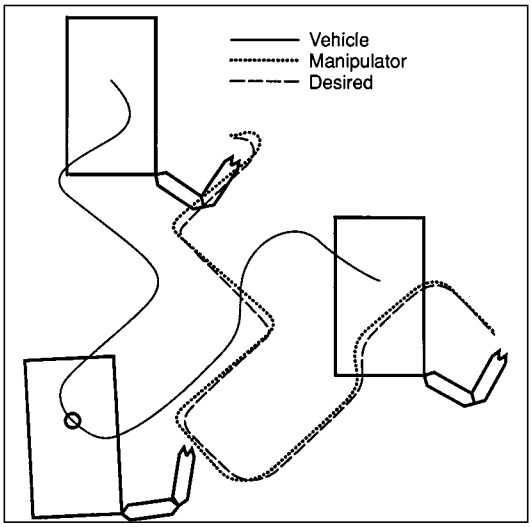

Figure 12: Performance using a coupled impedance controller with knowledge of coupled dynamics and capable of singularity avoidance.

Notice the higher fidelity with which the vehicle and the manipulator follow the desired trajectory. Despite only seeing the starting/intermediate/ending configurations of the system, one should be able to realize that this controller completely avoids singularities, while properly compensating for pitch-translation coupling. Even though the vehicle pitches through +/- 10 degrees, the manipulator compensates for it while avoiding singularities. This fact can be clearly visualized by comparing a much more abrupt desired trajectory as the one shown in Figure 13.

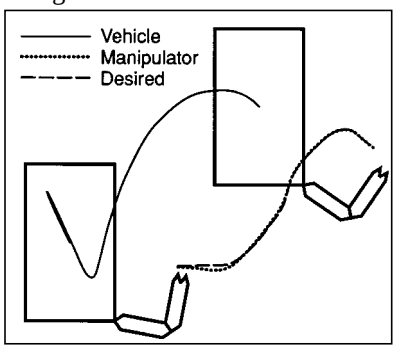

Figure 13: Performance using a coupled impedance controller indicating the motion co-ordination between vehicle and manipulator.

It is obvious that the vehicle performs a fairly noticeable recovery excursion towards the end of the commanded move, while the manipulator endpoint remains immobile. This implies that the manipulator completely compensated for the vehicle's behavior. The presence of the coupling impedance insured that no singularity was reached and that the relative vehicle-manipulator performance is well behaved.

V. OPERATIONAL SCENARIOS AND CRITERIA

The theoretical and simulation results need to be put into perspective from an operational standpoint. It is important to point out that this new coupled impedance structure allows for the use of a single input device, whose control coordinates need only minor (if any) re-mapping. Switching between different joysticks and operational modes is no longer necessary. The individual controller parameters such as stiffness, damping and inertia, can be selected to take advantage of the optimum vehicle response as a 'stiff' positioning platform, while the manipulator endpoint controller parameters are chosen depending on the task at hand. The operator could base changes in stiffness/damping/inertia on visual or tactile feedback, depending on the sophistication of the control-station's joystick/video setup. The coupling impedance between manipulator endpoint and the vehicle's focal point can be chosen to keep the orientation of the manipulator within a preferred workspace (maximize dexterity, center camera viewing point, etc.), or force the vehicle to respond only to large manipulator motions. From our experience we have found out, that all of these options are usually experimented with by the operator, who then selects a small number of possible parameter configurations and focal-point locations to perform the majority of his tasks. But the contingency is there to accommodate other more demanding tasks.

VI. CONCLUSIONS

The importance of careful design and nonlinear control schemes for underwater vehicle/manipulator systems control were presented. Understanding the implications of vehicle sensor, actuator, and packaging layout were explained by the need to minimize pitch/roll - translation coupling, while underscoring the importance of proper actuator models and controllers. In order to maximize stability and performance of vehicle/manipulator systems, a new coupling-impedance controller structure was presented which has a wide array of stability, robustness, and operational benefits over other currently employed techniques. Exploitation of the controller structure's benefits is maximized by proper model knowledge in the controller, in order to minimize vehicle/manipulator interactions, perform singularity avoidance, and increase the stability robustness margin. Simulation results were presented to support the above conclusions. Experimental work is currently underway to implement the above theory on an experimental vehicle/manipulator testbed[Yoerger and Ulrich].

VII. ACKNOWLEDGEMENTS

Dr. Neville Hogan at MIT was a continuing source of input during this research project. Drs. Kamal Youcef Toumi, Jean-Jacques Slotine and J. Kenneth Salisbury made valuable comments on the basic aspects of this research topic. This work was sponsored by the Office of Naval Research and the Office of Naval Technology, Contracts N00014-86-C-0038, N0-00014-87-J-1111, N000014-88-K-2022.

VIII. REFERENCES

1 Andrews, J. R.,"Impedance Control as a Framework for Implementing Obstacle Avoidance in a Manipulator", S.M. Thesis, Mech. Eng.'g., MIT, February 1983

2 Delonga, D. M.,"A Control System Design Technique for Nonlinear Discrete Time Systems", Ph.D. Thesis, MIT/WHOI Joint Program in Oceanographic Engineering, February 1989

3 BUSBY Associates, "Underwater Vehicles Directory", Arlington, VA, 1989

4 Yoerger, D.R., Cooke, J.G., Slotine, J.-J. E.,"The influence of Thruster Dynamics on Underwater Vehicle Behavior and their Incorporation into Control System Design", IEEE J. Oceanic Engineering, Vol. OE-15, (3), July 1990

5 Slotine, J.-J. E.,"Sliding Controller Design for Nonlinear Systems", Int. Journal of Control, Vol. 40(2), 1984

6 Slotine, J.-J. E., Coetsee, J.A.,"Adaptive Sliding Controller Synthesis for Nonlinear Systems", International Journal of Control, Vol. 42(6), 1986

7 Yoerger, D. R., Slotine, J.-J. E.,"Adaptive Sliding Control of an Experimental Underwater Vehicle", IEEE Int. Conf. on Robotics and Automation, 1991

8 DSL Design Team,"Design and Control of JASON", ROV 1988

9 Yoerger, D. R., et al,"Design of Underwater Vehicles for High Performance Control", ROV 1987

10 Yoerger, D. R., Von Alt, C., Bowen, A. D., Newman, J.,"JASON JR.: System Design and Deep Submergence Vehicle Interface", ROV 1987

11 Yoerger, D. R., Schempf, H., DiPietro, D.,"Design and Performance Evaluation of an Actively Compliant Underwater Manipulator for Full-Ocean Depth", Journal of Robotic Systems, 1991

12 Schempf, H.,"Coupled Dynamics of an Underwater Vehicle and its Impact on Design and Control", S.M. Thesis, Mechanical Engineering, MIT, 1986

13 Schempf, H.,"Impedance Control for Vehicle/Manipulator Systems", Deep Submergence Laboratory Report, WHOI/MIT Ph.D. Joint Program,Woods Hole, June 1, 1987

14 Schempf, H.,"Comparative Design, Modeling, and Control Analysis of Robotic Transmissions", Ph.D. Thesis, WHOI/MIT Ph.D. Joint Program in Mechanical and Oceanographic Engineering, Woods Hole and Cambridge, MA, August 1990

15 Yoerger, D. R., Slotine, J.-J. E.,"Task Resolved Motion Control of Vehicle-Manipulator Systems", IEEE Journal of Robotics and Automation, 2(2), 1987

16 DiPietro, D.,"Development of an Actively Compliant Underwater Manipulator", S.M. Thesis, MIT/WHOI Joint Program in Oceanographic Engineering, 1988

17 Hogan, N.,"Impedance Control: An Approach to Manipulation: Parts I, II and III", IEEE Journal of Dynamic Systems, Measurement and Control, 107, March 1985

18 Salisbury, J.K.,"Active Stiffness Control of a Manipulator in Cartesian Coordinates", 19th IEEE Conference on Decision and Control, Vol.1, Dec. 1980

19 Townsend, W. T., Salisbury, J. K.,"The Efficiency Limit of Belt and Cable Drives", ASME Journal of Mechanisms, Transmissions and Automation in Design, 1987

submitted to **International Federation of Automatic Control, CAMS'92,** Genova, Italy, 8-10 April 1992

COORDINATED VEHICLE/MANIPULATOR DESIGN AND CONTROL ISSUES FOR UNDERWATER TELEMANIPULATION

Hagen Schempf and Dana R. Yoerger[1]
Carnegie Mellon University
Robotics Institute - Field Robotics Center
5000 Forbes Ave., Pittsburgh, PA 15213, USA

ABSTRACT

Control of underwater vehicle/manipulator systems described by highly nonlinear and coupled dynamics can be improved through careful vehicle and manipulator design, while novel controller structures can improve system performance and simplify the man/machine interface requirements. Understanding and overcoming sensor limitations present in underwater vehicle navigation is one of the basic requirements for high fidelity control and trajectory planning of the manipulators' endeffector attached to its mobile base. Modelling and control of ducted propellers used as actuators becomes crucial for fine control and the avoidance of limit-cycling during hovering maneuvers. The ability to model the pitch/roll-translation coupling for such systems is necessary to increase the performance and fidelity of trajectory following and force/impedance control. Neglecting such coupling effects not only results in poor tracking performance but can also cause instabilities due to excitation of unmodelled 'pendulum' modes and the operation near vehicle/manipulator singularities. The necessity to coordinate vehicle and manipulator control for unconstrained motions and contact tasks requires the development of a coordinated controller structure. The use of a dual impedance structure can insure stability during contact tasks with a wide variety of environments, while the use of a coupling impedance is used to shape the relative behavior between vehicle and manipulator endpoint. The operational use of such a dual/coupled controller structure extends the maneuvering and manipulation capabilities of mobile manipulation platforms by reducing the number of variable controller parameters and thus operator burden while increasing system flexibility and userfriendliness of the man/machine interface. This paper presents preliminary simulation and experimental results.

I. INTRODUCTION

The use of manipulators on maintenance, recovery, and research ROVs has become standard practice. Such systems are usually controlled separately, in that there is a separate vehicle control joystick and another joystick/kinematic master to control the manipulator. The operational scenario usually involves getting to the work site and invoking a depth and/or heading servo on the vehicle so that the operator is free to concentrate on operating the robot arm. Other implementations may use a second arm to attach to a structure in order to stabilize the workplatform. This approach is usually not very common in research or recovery missions for ROVs, since there usually is no large fixed object to brace the vehicle against. The vehicle is usually required to free-float and compensate/coordinate motions with the manipulator.

Working off a mobile base which is gravity/buoyancy stabilized, while interacting with the environment, is not a very simple task. Not only will one need to coordinate vehicle and manipulator motions, but also the design of vehicle and manipulator have to be well thought out, as the inherent system dynamics may yield poor performance ('wobbly' base, swaying endeffector motions) and result in a poorly behaved or even unstable manipulator endeffector response.

The more recent design research and implementations for underwater vehicles [Schempf 1986], for use as camera platforms (JASON JUNIOR 1985) as well as manipulation platforms (JASON DESIGN 1988), have clearly stressed the important issues relevant to underwater vehicle design. Understanding such factors as (1) pitch/roll stabilization via metacentric height adjustments, (2) location of center of thrust and thrust allocation, (3) hydrodynamic cross-sections and center of drag, is important in the design of a stable workplatform, be it for imaging or manipulation tasks. The success of these designs for imaging purposes, was clearly illustrated in the 1986 TITANIC exploration with JASON Jr., and the last two JASON PROJECT explorations into the Mediterranean and Lake Ontario. In the last two cases, we were able to obtain clear and stable video images, while using additional sensors to accurately locate and identify archeologically valuable artifacts (amphoras, shipwreck outline, canons, masts, etc.) on two different shipwrecks (Roman shipwreck 400 A.D., and the Hamilton & Scourge from the Civil War). The quality of the video is substantially improved over that of other systems used for such tasks (AMUVS, Benthos RPV).

Manipulation off a platform such as JASON was also shown to be very successful, as the damageless recovery of 30 amphorae from 400 A.D., and biological and geological specimen

1: Deep Submergence Laboratory, Woods Hole Oceanographic Institution, Woods Hole, MA 02543, USA

from underwater 'smokers', have attested to. Not only vehicle design, but also careful manipulator and endeffector design proved to be crucial in this mission [DiPietro 1988, Yoerger et al 1989]. Designing a manipulator arm for dexterous and fine manipulation was necessary to be able to handle such delicate objects. Proper selection of motors and transmissions and sensors, including the proper control laws were all essential components of a successful implementation of a complete manipulation design and strategy, yielding a manipulator with superior performance, compared to other commercially available manipulators [Yoerger et al 1990, Schempf et al 1992].

The standard stiff position servos implemented on underwater electric and electro-hydraulic manipulators are not always sufficient to provide for fine, high dexterity and accurate control, where bandwidth and stability are important task performance criteria. Force-reflecting master/slave manipulators solve part of the problem, but deadbands, force thresholds and bandwidth limitations are again not always sufficient to yield acceptable performance. Insuring stability during interactive tasks, and good trajectory following can be accomplished with an impedance controller structure [Hogan 1985]. The use of such schemes has been proven to work very well on many stationary manipulators [Andrews 1983, Salisbury 1980], since it can be easily implemented in cartesian or task space, yielding desired spring-like and viscous damping behavior, with adjustable effective endpoint inertia. This approach gives the operator the ability to set desired behaviors which may be appropriate for different tasks. Prying a rock loose from an abatement may require 'stiff' joints (large stiffness and apparent mass), while handling an amphora or biological specimen would require a 'soft' apparent endpoint behavior (low stiffness, light apparent mass). We will show that this control technique can also be used to coordinate vehicle and manipulator motions, thereby combining stable control, endpoint behavior modulation and motion planning into a single structure. This approach extends the capabilities and handles provided by earlier task resolved controller designs [Yoerger & Slotine 1987].

Implementing such a stiffness or impedance control scheme on a manipulator mounted on a mobile base requires not only good knowledge of the dominant system dynamics (as they are rarely negligible), but also the restructuring of the control algorithm in order to coordinate vehicle and manipulator motions while insuring stability. Structuring the controller so as to yield the maximum performance versatility and ease of operation will result in a more operationally capable system. The complexity of the man/machine interface can be reduced from several physical system-specific input devices, to a single joystick or kinematic master, if a certain controller structure is selected with a minimal yet necessary set of controllable controller parameters.

This paper will first explore the important vehicle design and control issues involved in the design of a highly controllable workplatform. Constraints such as actuator and sensor limitations will be highlighted in order to understand and compensate for nonlinearities in pure vehicle control tasks. This will then be complemented by the study of the complex dynamics that dominate the dynamics of pitch/roll-translation for mobile underwater manipulation platforms. Modelling the coupled dynamics is necessary as even the best designed vehicle will pitch/roll and thus result in manipulator endpoint translations which have to be compensated for. The better our model of this physical system is, the better we can predict behavior and thus try to compensate for it. We will then explore the usefulness of the standard impedance and stiffness controller for redundant vehicle/manipulator systems and motivate the need for a modified impedance controller structure. The importance of proper dynamic modelling will become apparent when we compare the performance differences for different assumed model structures. A discussion of the important operational scenarios and criteria will also be given, in order to explain the ease and usefulness of such an implementation, while exploring the issues involved in controller parameter selection, as well as the implementation in simple task scenarios.

II. VEHICLE DESIGN AND CONTROL ISSUES

• *Vehicle Design Parameters (System Layout, Actuators and Sensors)*

The physical layout of the vehicle can have a very large impact on vehicle behavior [Schempf 1986, Yoerger et al 1986, DSL Design Team 1987]. The open-loop dynamics of the vehicle will have to be chosen so as to eliminate/reduce behaviors that are difficult to modify through feedback control and any available actuators. Vehicle pitch and roll have to be as passively stable as possible, by increasing the metacentric height (distance between the vehicle's center of gravity and center of buoyancy), which according to the simple pendulum's natural frequency equation $\omega = \sqrt{g/z_{cb-cg}}$ determines the frequency of oscillation [Tanaka et al 1985, Yoerger et al 1986, Schempf 1986]. The relation governing the maximum expected pitch/roll for a certain applied moment is

$$M_t + M_h = W z_{cb-cg} \sin\phi \qquad (1)$$

where:

M_t=Moment due to thruster(s)
M_h=Moment due to hydrodynamic effects
W= Dry Weight of the vehicle
z_{cb-cg}=Metacentric Height
ϕ=Pitch or Roll Angle

as shown in Eqn. 1. The applied moment M_t, can be upper-bounded by the moment created by the saturation thrust delivered by the forward/sideways thrusters, multiplied by the separation distance between center of thrust and the center of gravity. Keep in mind, that even if the center of thrust was perfectly aligned with the center of mass, the vehicle would still exhibit pitch/roll-translation coupling, due to the distributed added mass effects and the variable location of the net center of drag (captured by the term M_h).

Active control over these oscillatory modes can be obtained by proper placement of thrusters in a top-view triangular arrangement. The actuator saturation and geometrical characteristics really only allow for a limited amount of control, such as in aiding to damp out oscillations, but not to completely compensate for large pitch/roll excursions, because of external payload addition or coupling from an anchored manipulator exerting large forces. Careful placement of the thrusters is important, as it can minimize the pitch/roll-translation coupling due to the interactions of the center of thrust, center of drag and center-of-mass/center-of-thrust locations.

Ducted propellers driven by brushless DC motors, represent quite a nonideal actuator. Axial and cross-flows diminish thruster efficiency drastically, hampering control and maneuverability in the presence of any sizeable current.

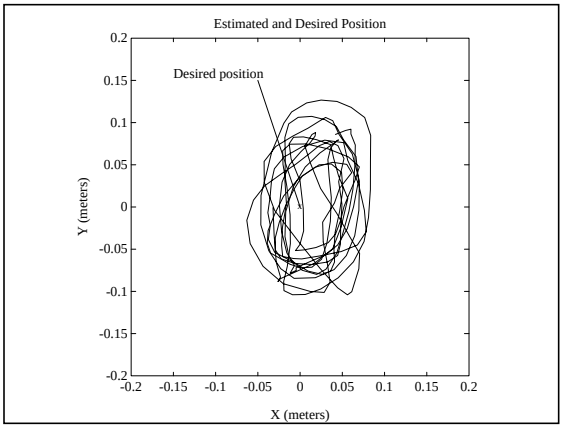

Figure 1: Limit-cycle phenomenon in a hovering ROV

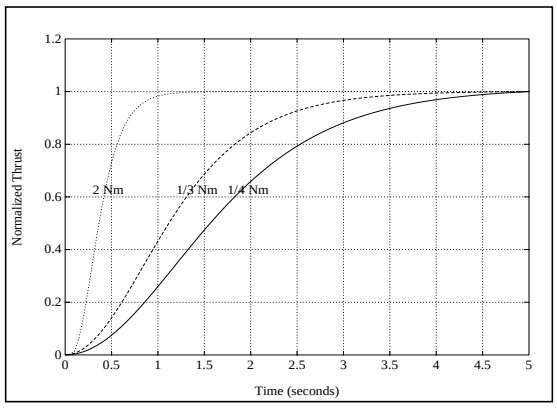

Figure 2: Nonlinear Thruster Characteristics

Seal- and motor-bearings affect the low-end thrust of the thruster, and cause the onset of 'hunting' during hovering maneuvers, akin to a steady limit-cycle about the desired position and heading (see Figure 1). It has been shown [Yoerger et al 1990], that the thruster behaves like a sluggish nonlinear filter, where the speed of response depends on the commanded thrust level (see Figure 2). A simple analysis showed that this results in a severe bandwidth limitation and causes limit cycles. The use of an adaptive sliding controller resulted in increased thruster fidelity and compensation for uncertainties in parameters and thruster degradation (broken prop. blade, fouling, etc.). The use of a model that parametrizes the thrust force as being proportional to the applied motor torque and the abs-square of the prop speed ($\omega|\omega|$), yields a structure that lent itself to an adaptive control and identification scheme. Performance improvements in hovering fidelity were achieved using this novel thruster model and adaptive controller.

The usual suite of sensors for underwater vehicles includes accelerometers, angular position and rate inclinometers, gyros, and depth and 3D acoustic positioning sensors. Heading and heading rate are usually measured by a flux-gate compass and a directional gyro. Heading measurements can be augmented and supported by placing two acoustic transponders separated along the vehicle and interrogating them within a high accuracy acoustic positioning net. Accuracies for a commercially available acoustic positioning net (SHARPS) can be as good as a few millimeters over a 120 meter range. This high frequency (300 kHz) acoustic system can deliver updates at about 10 Hz over its entire range. Accurate vehicle position updates are crucial in fine and high bandwidth vehicle and mobile manipulator control. The acoustic noise levels present at a certain work site can be 'filtered' without affecting update rate and accuracy. Blending all these independent and complimentary sensors is part of sensor fusion research currently underway, offering a good means of accounting for individual sensor accuracy, noise level, update rate and frequency response. A simple example would be the measurement of vehicle heading. One can blend the gyro (heading rate) measurements with that of the SHARPS (heading angle) system, by using a first order complimentary filter which produces a heading estimate that blends the accurate high frequency rate measurements of the gyro with those measurements from the accurate low frequency drift-free SHARPS system.

A drawing of the JASON system (Figure 3) illustrates the synthesis of many design criteria mentioned earlier. The shape and location of the flotation (syntactic foam), the location and distribution of vehicle components (weight distribution), the number and location of thrusters, and the location of acoustic transponders reflect some of the design decisions implemented in this remotely operated vehicle

platform.

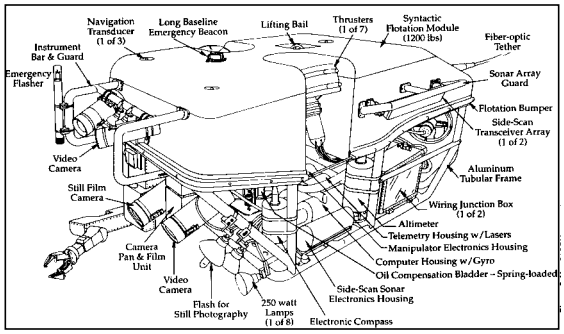

Figure 3: Layout View of JASON ROV

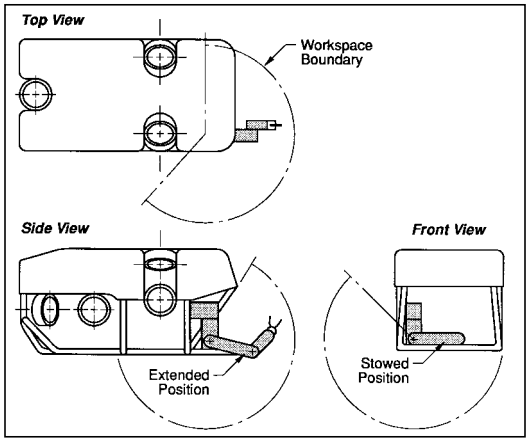

Figure 4: Plan Views of JASON's manipulator workspace

The attached manipulator arm was carefully placed with payload balancing and maximum available workspace in mind (see Figure 4). The importance of incorporating the manipulator into the kinematic and dynamic system model will be dealt with a bit later on in this paper, at which point we will illustrate the necessity and advantages to be gained.

• *Nonlinear Vehicle Dynamics*

Precise, reliable, and high bandwidth control of an underwater vehicle requires the synthesis of solutions to challenging problems in vehicle design, sensing, dynamic modelling and control system design. The dynamics of such systems are very hard to characterize deterministically for several reasons. Physically, the usually unstreamlined, non-hydrodynamic shape of these vehicles, results in hydrodynamic drag and added/effective mass effects which are difficult to model. A model structure is based mainly on empirically derived relations, such as the abs-square drag law ($u|u|$) with a variable drag coefficient or the acceleration-dependent added mass term, and even then such nonlinear expressions have parameters that are not fixed, but vary as a function of many other parameters. The most commonly used nonlinear model

$$\Sigma \vec{F} = \hat{\underline{M}}_e \ddot{\vec{x}} = \hat{\alpha} \vec{F}_u - \hat{\underline{C}}_d \dot{x}|\dot{x}| + \hat{\underline{F}}_d \qquad (2)$$

where:

F_u=Actuator Thrust
F_d=Disturbance Forces (currents, tether,...)
C_d=Drag Coefficient
M_e=Effective Inertia Tensor
α=Actuator Gain
x=Linear Displacement

structure is shown in Eqn.2, using Newton's laws to express the behavior of the vehicle as a function of best-estimate parameters (denoted by '^') in the drag term C_d, the effective mass M_e, the disturbance F_d, and the actuator gain α. Bounding the uncertainty in the knowledge of these terms as well as that of the disturbance-term F_d, can be effectively used in sliding control [Slotine 1985], to design a robust controller and thus improve overall system performance without the need for time and money-consuming hydrodynamic modelling and the subsequent design of gain-scheduling controllers. Performance in closed-loop trials has been shown to be better and more robust than with other standard controller structures. Figure 5 illustrates this point by showing a top-view of a closed-loop rectangular trajectory-following task for the BENTHOS ROV.

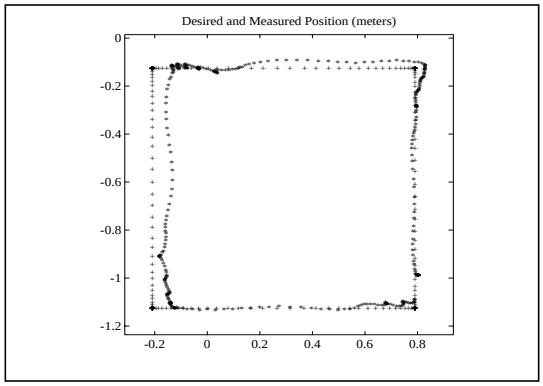

Figure 5: Closed-loop ROV trajectory following performance

More recent work [Yoerger 1990, 1991] has also shown that one can use adaptive techniques to continuously update estimates of effective mass, actuator gain, disturbances, and drag coefficient, as denoted in Eqn.3 by the time-variation symbol 't', to improve system performance and even obtain better physical estimates of these parameters.

$$\hat{\underline{M}}_e(t)\ddot{\vec{x}} = \hat{\alpha}(t)\vec{F}_u - \hat{\underline{C}}_d(t)\dot{x}|\dot{x}| + \hat{\underline{F}}_d(t) \qquad (3)$$

Shown in figure 6, we can illustrate adaptation convergence for the different parameters (added mass, drag coefficient, actuator gain) through a single error-metric plot. Sliding control methodologies [Yoerger and Slotine, 1988] will insure that adaptation will force the error-metric to eventually remain within deterministic boundaries, as shown in figure 6. This approach represents a viable solution to operations in highly variable underwater currents, or scenarios where disturbances due to tether drag are not uncommon nor negligible. Since we simplified the hydrodynamics of the system, neglecting

vortex shedding and past fluid flow history, we can at least expect, if properly bounded, that the ensuing disturbances can be compensated for in an optimum and robust fashion. A discrete nonlinear implementation of the above system dynamics and subsequent controller development are treated in detail by Delonga [1987].

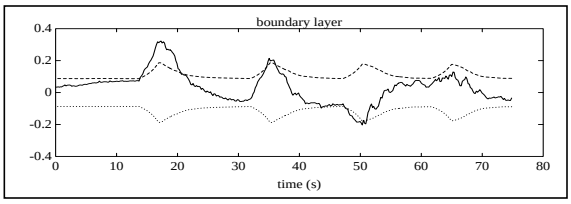

Figure 6: Convergence of error-metric 's' to within achievable boundaries..

III. VEHICLE - MANIPULATOR DYNAMICS

In order to understand the complexities involved in the dynamics and control issues of vehicle/manipulator systems, consider the system depicted in Figure 7. We have shown a vehicle and its manipulator as a 3-dimensional system, with 5 degrees of freedom. The vehicle is allowed to translate forward and in reverse, change vertical position up and down, while allowing for pitching motions. The 2 DOF manipulator remains in the *uw*-plane described by the vehicle coordinates. Notice that the translational vehicle velocities are described in a body-referenced frame. We have limited ourselves to such a system in order to illustrate the problems one encounters while attempting to design a controller for such a highly coupled system.

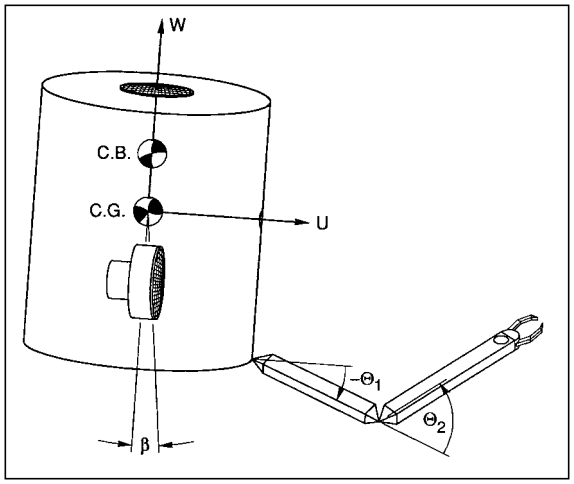

Figure 7: Vehicle/Manipulator System with 5 degrees of freedom moving in the vertical plane.

The complexity of the model can be increased by including another set of coupled/uncoupled equations to study the roll/translation dynamics. We will limit ourselves in this study to pitch-translation coupling.

The physical system can now be modelled by a set of parameters to be used in the Lagrangian expression in order to derive the equations of motion using the required set of generalized coordinates.

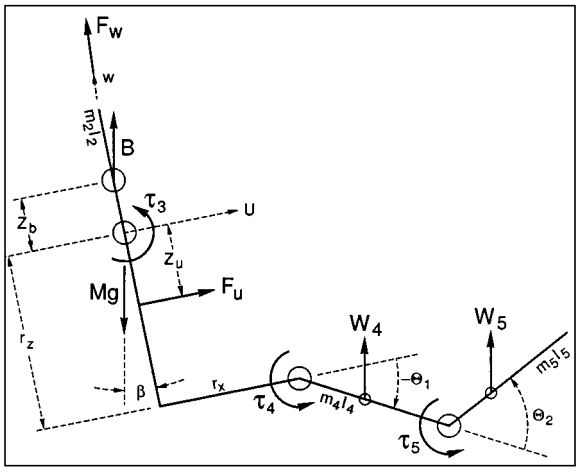

Figure 8: Parametric stick-figure showing modelling parameters.

Figure 8 illustrates these in a stick figure with parameters and variables necessary to assemble the Lagrangian, which consists of kinetic and potential co-energy terms:

$$L=T^{*} - U, \text{ where}$$

$$\text{and, } U = \sum_{i=1}^{n} m_i \vec{g}^{T} r_{o,ci} \qquad (4)$$

Using body-referenced vehicle translation velocities u and w, vehicle pitch angle β and rate q, and the manipulator coordinate angles θ_1 and θ_2 with rates $\delta(\theta_1)/dt$ and $\delta(\theta_2)/dt$ as the generalized coordinates Θ, we can formulate the Lagrangian energy terms. Using the rules for generating the individual equations of motion

$$\frac{d}{dt}\frac{\partial L}{\partial \dot{\Theta}_i} - \frac{\partial L}{\partial \Theta_i} = Q_i \ldots i = 1, \ldots, n \qquad (5)$$

we arrive at a set of equations, which in vector for can be written as:

$$\underline{H}(\vec{\Theta})\,\ddot{\vec{\Theta}} + \vec{h}(\dot{\vec{\Theta}}, \vec{\Theta}, t) = \vec{\tau}$$

$$where \ldots \dot{\vec{\Theta}} = \begin{bmatrix} u & w & q & \dot{\theta}_1 & \dot{\theta}_2 \end{bmatrix}^{T} \qquad (6)$$

The individual components of the inertia tensor $\underline{H}(\vec{\Theta})$, are made up of the individual inertia terms as well as several cross-coupling

terms, which result in a symmetric matrix. In order to understand that even in the inertia tensor the cross-coupling effects are not negligible, we analyzed the absolute magnitude representation of the individual elements of the inertia matrix (assumes sin(?)~1 and cos(?)~1), which represent the coupling of the vehicle accelerations (u, v, q) and the manipulator (θ_1, θ_2). Remember that the linear manipulator endpoint accelerations are influenced by the angular accelerations of the vehicle ($H_{(1,2)3}$), as well as the joint accelerations ($H_{(1,2)(4,5)}$), and vice versa. Depending on the physical parameters m_4, m_5, l_4, l_{c4}, l_5 and l_{c5}, the cross-coupling effects will vary in magnitude. If we assume that for a typical underwater vehicle/manipulator system, the inertia ratio M/m lies around 20:1, with a workspace of about 2 meters, and vehicle dimensions such that $r_x=r_z=1$ meter, we can get a matrix scaling effect such that the inertia matrix magnitudes can be numerically expressed as:

$$\underline{H} \cong M \begin{bmatrix} 1.1 & 0 & 0.2 & 0.1 & 0.025 \\ 0 & 1.1 & 0.2 & 0.1 & 0.025 \\ 0.2 & 0.2 & 1.45 & 0.45 & 0.225 \\ 0.1 & 0.1 & 0.45 & 0.213 & 0.2 \\ 0.025 & 0.025 & 0.225 & 0.2 & 0.075 \end{bmatrix} \quad (7)$$

Notice that the coupling magnitudes between translation and pitch motions are quite pronounced. Coupling between linear accelerations and rotary manipulator-link accelerations can also be quite substantial. The above analysis thus illustrates that including these modes into the overall system dynamics is well justified and that they should thus be incorporated into the controller design to yield improved performance and bandwidth.

The nonlinear cross-coupling terms assembled in $\underline{R}\left(\dot{\bar{\Theta}}, \bar{\Theta}\right)$ contain multiplicative terms in $u\dot{\theta}_1, u\dot{\theta}_2, w\dot{\theta}_1, w\dot{\theta}_2, q\dot{\theta}_1, q\dot{\theta}_2, \dot{\theta}_1^2, \dot{\theta}_2^2, \dot{\theta}_1\dot{\theta}_2, q^2, uq, wq$, and thus represent coupling terms whose magnitudes can also be shown to introduce substantial cross-coupling dynamics into all degrees of freedom. Ignoring the uq, wq, q^2, and $q\theta_{1,2}$ terms that show up in the equations for the manipulator link dynamics, could reduce closed-loop performance (bandwidth) and even represent a source of instability in a controller design which omits this coupling at the modelling stage.

The generalized forcing terms τ, are comprised of not only the actuator efforts F_u and F_w, but also the buoyancy restoring torque due to a nonzero metacentric height, and the effective drag terms on the vehicle and manipulator link geometries [Schempf 1986]. At this point the possibility to add active pitch control to the vehicle to offset the coupling of the fore/aft thruster moment about the center of gravity ($F_u z_u$), offers a possibility for the study in actuator placement, saturation characteristics and cost/performance trade-offs.

The entire details of the equations of motion are omitted here, since the actual goal of this paper is to study the use of different controller structures and their effect on closed-loop performance. The importance of this derivation, lies in emphasizing the retention of those terms that are not negligible, since they are responsible for the coupling dynamics that dominate the behavior of closed loop controlled vehicle/manipulator systems (see [Schempf 1987] for a more detailed analysis).

IV. CONTROLLER STRUCTURES

We have analyzed and experimentally compared several different controller structures which were designed and implemented separately for a vehicle and its manipulator. The performance was many times limited due to vehicle/manipulator interactions, and the combination of vehicle servoing and active joystick control of the manipulator was quite cumbersome and did not always result in desirable performance. A more complex yet beneficial controller structure was then proposed and can best be represented by the drawing in Figure 9. It shows an underwater vehicle/manipulator robot, with desired endpoint and vehicle behaviors w.r.t. the desired position represented as springs. Notice that we now have a controller that will attempt to control the endpoint of the manipulator and a fictitious vehicle point - termed the 'focal point' here - to track a desired trajectory indicated by x_d, y_d, and z_d which are cartesian positions, represented by the vector $\underline{X}_o$. A single controller is thus capable of controlling all subsystems, with behaviors that are described by the desired closed-loop system descriptors such as stiffness, damping, and inertia.

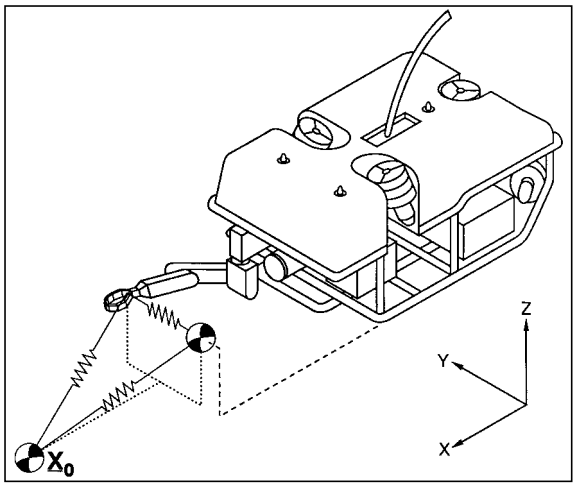

Figure 9: Coupling Impedance Controller Structure for an underwater vehicle/manipulator system.

Proper selection of these controller parameters and the respective location of the 'focal point' could allow for all possible desired vehicle and endeffector behaviors necessary to accomplish a certain task. The importance of including the proper system model into the controller was explored by simulating the 5 DOF system of Figure 7, and including in the

controller different levels of model sophistication. The analysis covers three different types of controller structures; the first which treats manipulator and vehicle as two completely separate and un-coupled systems, the second which incorporates coupled dynamics, but does not attempt to coordinate vehicle nor manipulator responses, and lastly a complete controller structure like the one in Figure 9 with knowledge of the coupling dynamics. All simulations were run with about a 25% error in model parameters, and with response bandwidths typical to the systems being analyzed (vehicle ~ 1-2 Hz, and manipulator ~ 10-15 Hz). The simulation results are graphically depicted to highlight system behavior more clearly.

• *Decoupled, reduced-order controllers*

If two separate controllers were implemented on a vehicle/manipulator system, and tuned to maximize the performance of their respective platforms, one can show that performance and even stability can be compromised in a coordinated motion. To illustrate this argument, one can command a parallel trajectory to the manipulator and vehicle and then implement those controllers, with results as shown in Figure 10.

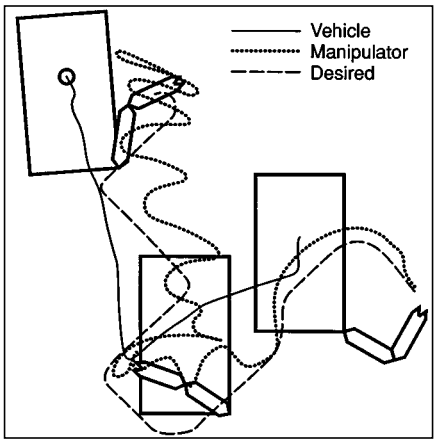

Figure 10: Performance using a controller without knowledge of coupled dynamics nor singularities

Notice the low-pass filtered response of the vehicle, coupled with excessive tracking errors for the manipulator endpoint due to pitch-translation interactions, and the constant crossing of singularity configurations of the manipulator, resulting in extremely undesirable system response. Depicted in Figure 10 are the starting, ending, and intermediate configurations of the vehicle/manipulator system. Based on this suboptimum response, one would conclude that the first improvement should be sought by including knowledge of the coupled dynamics within the controller and thus attempt to compensate for them - the approach taken and illustrated next.

• *Decoupled high-order controllers*

We have increased the controller complexity by incorporating in each separate controller knowledge about the coupling and the resulting forces/torques generated due to the interactions. As one would expect, the highly oscillatory behavior due to pitch/translation interactions has been removed, yet the trajectory tracking is still not satisfactory, which can be traced to the continuous proximity of the manipulator to its singular configurations - notice that it even reaches 'into' the vehicle, which is obviously not desirable (see Figure 11).

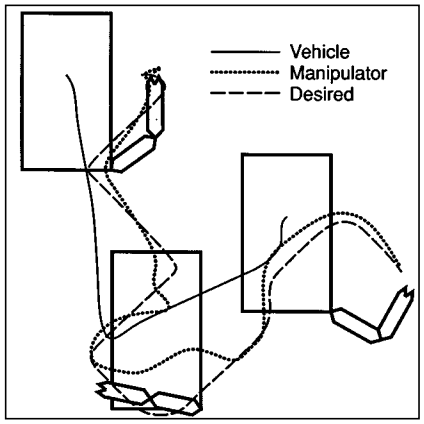

Figure 11: Performance using a controller with knowledge of coupled dynamics but without the ability to compensate for singularities.

We have now established the proper motivation for the controller structure shown in Figure 9, with the characteristic performance outlined next.

• *Coupled impedance controller*

The selected controller structure allows for a single controller to control both subsystems based on a desired trajectory to be followed by the vehicle and the manipulator endpoint. This controller structure need not know about the coupled dynamics to work properly, but its performance and stability margin are vastly improved if the coupling dynamics are included explicitly. The performance of the coupled system is depicted in Figure 12.

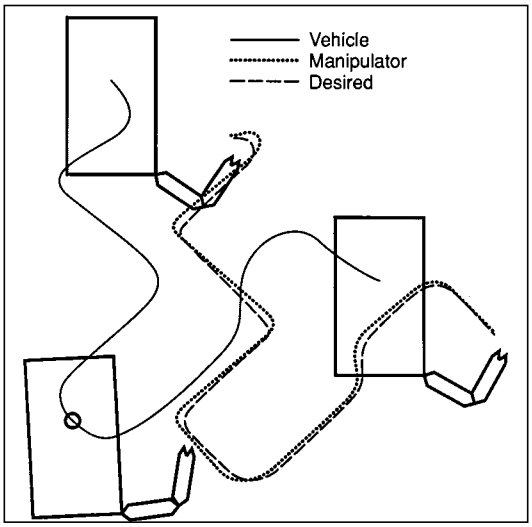

Figure 12: Performance using a coupled impedance controller with knowledge of coupled dynamics and capable of singularity avoidance.

Notice the higher fidelity with which the vehicle and the manipulator follow the desired trajectory. Despite only seeing the starting/intermediate/ending configurations of the system, one should be able to realize that this controller completely avoids singularities, while properly compensating for pitch-translation coupling. Even though the vehicle pitches through +/- 10 degrees, the manipulator compensates for it while avoiding singularities. This fact can be clearly visualized by comparing a much more abrupt desired trajectory as the one shown in Figure 13.

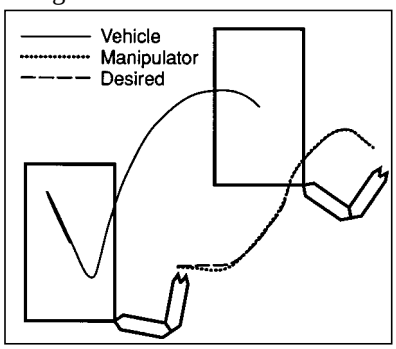

Figure 13: Performance using a coupled impedance controller indicating the motion co-ordination between vehicle and manipulator.

It is obvious that the vehicle performs a fairly noticeable recovery excursion towards the end of the commanded move, while the manipulator endpoint remains immobile. This implies that the manipulator completely compensated for the vehicle's behavior. The presence of the coupling impedance insured that no singularity was reached and that the relative vehicle-manipulator performance is well behaved.

V. OPERATIONAL SCENARIOS AND CRITERIA

The theoretical and simulation results need to be put into perspective from an operational standpoint. It is important to point out that this new coupled impedance structure allows for the use of a single input device, whose control coordinates need only minor (if any) re-mapping. Switching between different joysticks and operational modes is no longer necessary. The individual controller parameters such as stiffness, damping and inertia, can be selected to take advantage of the optimum vehicle response as a 'stiff' positioning platform, while the manipulator endpoint controller parameters are chosen depending on the task at hand. The operator could base changes in stiffness/damping/inertia on visual or tactile feedback, depending on the sophistication of the control-station's joystick/video setup. The coupling impedance between manipulator endpoint and the vehicle's focal point can be chosen to keep the orientation of the manipulator within a preferred workspace (maximize dexterity, center camera viewing point, etc.), or force the vehicle to respond only to large manipulator motions. From our experience we have found out, that all of these options are usually experimented with by the operator, who then selects a small number of possible parameter configurations and focal-point locations to perform the majority of his tasks. But the contingency is there to accommodate other more demanding tasks.

VI. CONCLUSIONS

The importance of careful design and nonlinear control schemes for underwater vehicle/manipulator systems control were presented. Understanding the implications of vehicle sensor, actuator, and packaging layout were explained by the need to minimize pitch/roll - translation coupling, while underscoring the importance of proper actuator models and controllers. In order to maximize stability and performance of vehicle/manipulator systems, a new coupling-impedance controller structure was presented which has a wide array of stability, robustness, and operational benefits over other currently employed techniques. Exploitation of the controller structure's benefits is maximized by proper model knowledge in the controller, in order to minimize vehicle/manipulator interactions, perform singularity avoidance, and increase the stability robustness margin. Simulation results were presented to support the above conclusions. Experimental work is currently underway to implement the above theory on an experimental vehicle/manipulator testbed[Yoerger and Ulrich].

VII. ACKNOWLEDGEMENTS

Dr. Neville Hogan at MIT was a continuing source of input during this research project. Drs. Kamal Youcef Toumi, Jean-Jacques Slotine and J. Kenneth Salisbury made valuable comments on the basic aspects of this research topic. This work was sponsored by the Office of Naval Research and the Office of Naval Technology, Contracts N00014-86-C-0038, N0-00014-87-J-1111, N000014-88-K-2022.

VIII. REFERENCES

1 Andrews, J. R.,"Impedance Control as a Framework for Implementing Obstacle Avoidance in a Manipulator", S.M. Thesis, Mech. Eng.'g., MIT, February 1983

2 Delonga, D. M.,"A Control System Design Technique for Nonlinear Discrete Time Systems", Ph.D. Thesis, MIT/WHOI Joint Program in Oceanographic Engineering, February 1989

3 BUSBY Associates, "Underwater Vehicles Directory", Arlington, VA, 1989

4 Yoerger, D.R., Cooke, J.G., Slotine, J.-J. E.,"The influence of Thruster Dynamics on Underwater Vehicle Behavior and their Incorporation into Control System Design", IEEE J. Oceanic Engineering, Vol. OE-15, (3), July 1990

5 Slotine, J.-J. E.,"Sliding Controller Design for Nonlinear Systems", Int. Journal of Control, Vol. 40(2), 1984

6 Slotine, J.-J. E., Coetsee, J.A.,"Adaptive Sliding Controller Synthesis for Nonlinear Systems", International Journal of Control, Vol. 42(6), 1986

7 Yoerger, D. R., Slotine, J.-J. E.,"Adaptive Sliding Control of an Experimental Underwater Vehicle", IEEE Int. Conf. on Robotics and Automation, 1991

8 DSL Design Team,"Design and Control of JASON", ROV 1988

9 Yoerger, D. R., et al,"Design of Underwater Vehicles for High Performance Control", ROV 1987

10 Yoerger, D. R., Von Alt, C., Bowen, A. D., Newman, J.,"JASON JR.: System Design and Deep Submergence Vehicle Interface", ROV 1987

11 Yoerger, D. R., Schempf, H., DiPietro, D.,"Design and Performance Evaluation of an Actively Compliant Underwater Manipulator for Full-Ocean Depth", Journal of Robotic Systems, 1991

12 Schempf, H.,"Coupled Dynamics of an Underwater Vehicle and its Impact on Design and Control", S.M. Thesis, Mechanical Engineering, MIT, 1986

13 Schempf, H.,"Impedance Control for Vehicle/Manipulator Systems", Deep Submergence Laboratory Report, WHOI/MIT Ph.D. Joint Program,Woods Hole, June 1, 1987

14 Schempf, H.,"Comparative Design, Modeling, and Control Analysis of Robotic Transmissions", Ph.D. Thesis, WHOI/MIT Ph.D. Joint Program in Mechanical and Oceanographic Engineering, Woods Hole and Cambridge, MA, August 1990

15 Yoerger, D. R., Slotine, J.-J. E.,"Task Resolved Motion Control of Vehicle-Manipulator Systems", IEEE Journal of Robotics and Automation, 2(2), 1987

16 DiPietro, D.,"Development of an Actively Compliant Underwater Manipulator", S.M. Thesis, MIT/WHOI Joint Program in Oceanographic Engineering, 1988

17 Hogan, N.,"Impedance Control: An Approach to Manipulation: Parts I, II and III", IEEE Journal of Dynamic Systems, Measurement and Control, 107, March 1985

18 Salisbury, J.K.,"Active Stiffness Control of a Manipulator in Cartesian Coordinates", 19th IEEE Conference on Decision and Control, Vol.1, Dec. 1980

19 Townsend, W. T., Salisbury, J. K.,"The Efficiency Limit of Belt and Cable Drives", ASME Journal of Mechanisms, Transmissions and Automation in Design, 1987